Loss of p57KIP2 expression confers resistance to contact inhibition in human androgenetic trophoblast stem cells

	Sota Takahashi, Hiroaki Okae, Norio Kobayashi, Akane Kitamura, Kanako Kumada, Nobuo Yaegashi, Takahiro Arima
journal or publication title	Proceedings of the National Academy of Sciences of the United States of America
volume	116
number	52
page range	26606-26613
year	2019-12-26
URL	http://hdl.handle.net/10097/00130746

Loss of p57^{KIP2} expression confers resistance to contact inhibition in human androgenetic trophoblast stem cells

Sota Takahashi[a,1], Hiroaki Okae[a,1,2], Norio Kobayashi[a], Akane Kitamura[a], Kanako Kumada[a], Nobuo Yaegashi[b], and Takahiro Arima[a,2]

[a]Department of Informative Genetics, Environment and Genome Research Center, Tohoku University Graduate School of Medicine, Aoba-ku, 980-8575 Sendai, Japan; and [b]Department of Obstetrics and Gynecology, Tohoku University Graduate School of Medicine, Aoba-ku, 980-8575 Sendai, Japan

A complete hydatidiform mole (CHM) is androgenetic in origin and characterized by enhanced trophoblastic proliferation and the absence of fetal tissue. In 15 to 20% of cases, CHMs are followed by malignant gestational trophoblastic neoplasms including choriocarcinoma. Aberrant genomic imprinting may be responsible for trophoblast hypertrophy in CHMs, but the detailed mechanisms are still elusive, partly due to the lack of suitable animal or in vitro models. We recently developed a culture system of human trophoblast stem (TS) cells. In this study, we apply this system to CHMs for a better understanding of their molecular pathology. CHM-derived TS cells, designated as TS^{mole} cells, are morphologically similar to biparental TS (TS^{bip}) cells and express TS-specific markers such as GATA3, KRT7, and TFAP2C. Interestingly, TS^{mole} cells have a growth advantage over TS^{bip} cells only after they reach confluence. We found that p57^{KIP2}, a maternally expressed gene encoding a cyclin-dependent kinase inhibitor, is strongly induced by increased cell density in TS^{bip} cells, but not in TS^{mole} cells. Knockout and overexpression studies suggest that loss of p57^{KIP2} expression would be the major cause of the reduced sensitivity to contact inhibition in CHMs. Our findings shed light on the molecular mechanism underlying the pathogenesis of CHMs and could have broad implications in tumorigenesis beyond CHMs because silencing of p57^{KIP2} is frequently observed in a variety of human tumors.

complete hydatidiform mole | genomic imprinting | trophoblast stem cells | p57KIP2 | choriocarcinoma

A complete hydatidiform mole (CHM) is a gestational trophoblastic disease characterized by enhanced trophoblast proliferation, swollen villi, and the absence of embryonic components (1). Whereas the core mesenchyme of normal villi is surrounded by a single layer of cytotrophoblast (CT) cells, CHM villi contain multiple layers (2). Although CHMs are benign in most cases, 15 to 20% of them are followed by malignant gestational trophoblastic neoplasms, including invasive mole and choriocarcinoma (3). CHMs develop from androgenetic conceptuses (4, 5) and can be placed into 2 classes: monospermic and dispermic. The majority of CHMs are monospermic and arise from fertilization of an anucleate egg with a haploid sperm, followed by endoreduplication. Dispermic CHMs account for 4 to 15% of CHMs and develop through fertilization of an anucleate egg with 2 sperm (6).

Whereas most autosomal genes are expressed from both parental alleles, a small subset of genes, known as imprinted genes, are exclusively expressed from 1 parental allele (7). To date, more than 100 imprinted genes have been identified in humans (8), and many of them are expressed in the placenta (9). Aberrant genomic imprinting may be responsible for the pathogenesis of CHMs. However, it remains uncertain which imprinted gene(s) are involved in the overgrowth of trophoblast cells in CHMs, partly due to the lack of suitable animal or in vitro models. For example, androgenetic mouse embryos exhibit severe growth retardation and early lethality. The extraembryonic tissues develop relatively well in these embryos but do not give rise to malignant trophoblastic neoplasms (10, 11). Moreover, some immortalized cell lines have been established from CHMs by transducing oncogenes such as human telomerase reverse transcriptase (12, 13), but forced expression of oncogenes affects cell proliferation and can mask the phenotype of CHMs.

Recently, we have succeeded in establishing human trophoblast stem (TS) cells from cytotrophoblast (CT) cells isolated from first-trimester placentas (14). Here, we apply this culture system to CHMs and reveal that CHM-derived TS cells exhibit resistance to contact inhibition, which may be accounted for by loss of p57^{KIP2} (CDKN1C) expression. These findings are fundamental to understanding the pathogenesis of CHMs and normal placental development.

Results

Establishment and Molecular Characterization of TS Cells from CHMs. We isolated CT cells from 5 CHM samples and established TS cell lines (Fig. 1A and SI Appendix, Table S1). These cells, designated as TS^{mole} cells, were morphologically similar to

---

Significance

Complete hydatidiform moles (CHMs) develop from androgenetic conceptuses and are characterized by enhanced proliferation of trophoblast cells and a significantly higher risk of trophoblast tumors. Loss of the maternal genome and duplication of the paternal genome are considered to be responsible for the phenotype, but the detailed mechanism remains unclear. Here, we report the derivation of trophoblast stem (TS) cells from CHMs. These cells have reduced sensitivity to contact inhibition of cell proliferation and exhibit aberrant expression of imprinted genes, which are expressed from only 1 parental allele. We also reveal that the maternally expressed imprinted gene p57^{KIP2} would be responsible for the enhanced proliferation of CHM-derived TS cells. Our findings provide an insight into the pathogenesis of CHMs.
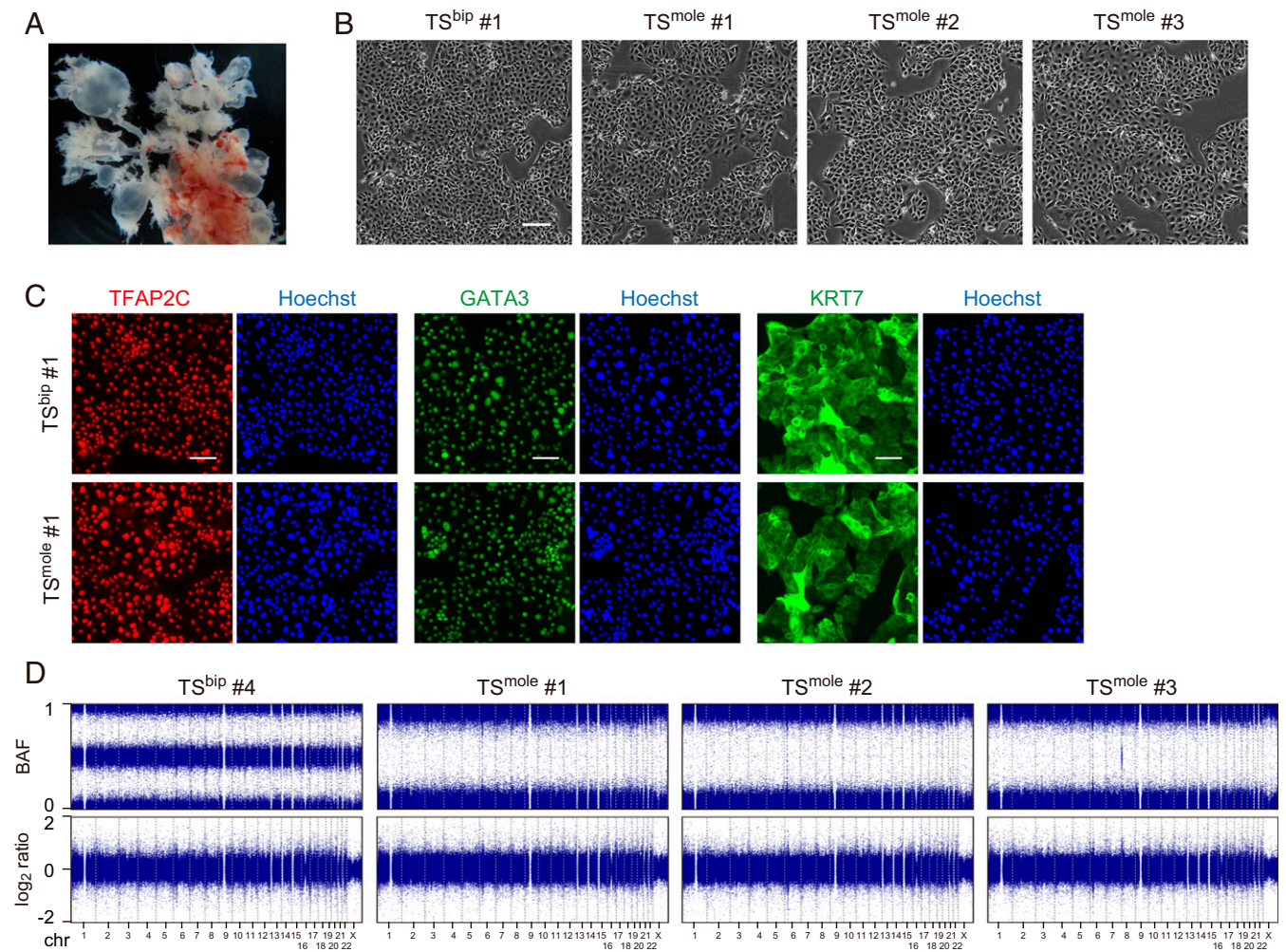

Fig. 1. Establishment of TS^mole cells. (*A*) Representative CHM image. Swollen villi are visible. (*B*) Phase-contrast images of TS^bip and TS^mole cells. (*C*) Immunostaining of TFAP2C, GATA3, and KRT7. Nuclei were counterstained with Hoechst 33258. (*D*) CNV analysis of TS^bip and TS^mole cells. B allele frequency (BAF) and log$_2$ copy number ratio (log$_2$ ratio) are shown. Genome-wide loss of heterogeneity was observed in TS^mole cell lines without copy number changes. (Scale bars: *B*, 200 μm; *C*, 100 μm.)

biparental TS (TS^bip) cells (Fig. 1*B*) and expressed trophoblast markers such as TFAP2C, GATA3, and KRT7 (Fig. 1*C*). We performed copy number variation (CNV) analysis of 3 TS^mole cell lines with the Japonica array, which is a SNP array optimized for the Japanese population, and revealed genome-wide loss of heterogeneity (Fig. 1*D*). Thus, these 3 lines may be derived from monospermic fertilization.

To further characterize TS^mole cells, we performed RNA sequencing (RNA-seq) and whole genome bisulfite sequencing (WGBS) on 3 TS^mole cell lines. RNA-seq and WGBS data for TS^bip cells were obtained from our previous study and used for comparison (14). TS^mole and TS^bip cells had very similar transcriptome and methylome profiles, and the expression levels of differentiation markers were low in these cells (*SI Appendix,* Fig. S1 and Dataset S1). However, expression and DNA methylation of imprinted genes were disturbed in TS^mole cells (Fig. 2*A* and Dataset S2). We focused on 10 maternally expressed and 15 paternally expressed genes that maintain allele-specific expression in primary CT cells (15). Among the maternally expressed genes, *H19* and *p57^KIP2* were expressed at the lowest level in TS^mole cells compared to TS^bip cells. Consistently, the paternally methylated *H19* DMR was hypermethylated and the maternally methylated KvDMR1 was unmethylated in TS^mole cells (Fig. 2 *C* and *D*). KvDMR1 overlaps with the promoter of the paternally

expressed noncoding RNA *KCNQ1OT1*, which may be involved in the repression of neighboring genes such as *KCNQ1* and *p57^KIP2* (16). However, several maternally expressed genes, such as *NAA60* and *GRB10*, showed comparable expression levels in TS^mole and TS^bip cells (Fig. 2*A*). This was unlikely to be due to an artifact of in vitro culture because the expression levels of *NAA60* and *GRB10* were also similar between primary CT cells isolated from CHMs and normal placentas (Fig. 2*B*).

We also revealed that paternally expressed genes with high expression levels in TS^bip cells tended to show increased expression in TS^mole cells (Fig. 2*A*). However, several genes, including *PEG3* and *AIM1*, did not show increased expression in TS^mole cells, which was inconsistent with the methylation patterns of their regulatory elements (Fig. 2 *E* and *F*). Intriguingly, increased expression of paternally expressed genes was less apparent in primary CT cells isolated from CHMs (Fig. 2*B*). Although we analyzed only 2 CT samples from CHMs and more samples are needed to draw a firm conclusion, these data suggest that there may be a compensatory mechanism whereby the expression levels of some imprinted genes are normalized in CHMs. Such a mechanism might also work in TS^mole cells but to a lesser extent.
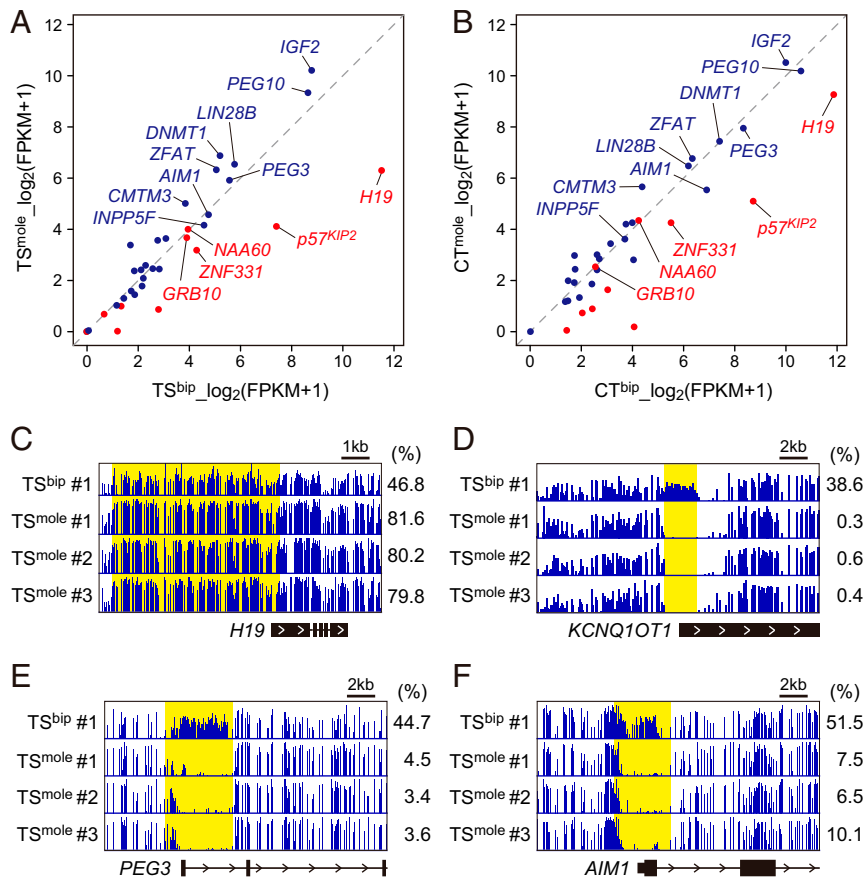
Takahashi et al.

CELL BIOLOGY

Fig. 2. RNA-seq and WGBS of TS^{mole} cells. (*A*) Expression levels of imprinted genes in TS^{bip} and TS^{mole} cells. Three lines were analyzed for each cell type, and mean expression levels are shown. Maternally and paternally expressed genes are represented in red and blue, respectively. Genes with >10 FPKM in TS^{bip} cells are labeled with their gene names. (*B*) Expression levels of imprinted genes in CT cells isolated from biparental placentas (CT^{bip}) and CHMs (CT^{mole}). Three CT^{bip} and two CT^{mole} samples were analyzed, and mean expression levels are shown. Genes are labeled as in *A*. (*C*) DNA methylation patterns at the *H19* DMR. The *H19* DMR is shown in yellow, and its methylation levels are indicated on the right. (*D*) DNA methylation patterns at KvDMR1 (yellow). (*E*) DNA methylation patterns at the *PEG3* DMR (yellow). (*F*) DNA methylation patterns at the *AIM1* DMR (yellow). See also Datasets S1 and S2.

Resistance to Contact Inhibition in TS^{mole} Cells. Since CHMs are characterized by trophoblast hypertrophy, we analyzed the proliferation rate of TS^{mole} cells. However, TS^{mole} cells had a proliferation rate comparable to TS^{bip} cells under optimal conditions where the cells were passaged before they reached confluence (Fig. 3*A*). It has been recognized that although the core mesenchyme of normal villi is surrounded by a single layer of CT cells, CHM villi contain multiple layers (2). This implies that trophoblast cells of CHMs might be resistant to contact inhibition of proliferation. Consistent with this, we found that TS^{mole} cells had a significant growth advantage over TS^{bip} cells after they reached confluence (Fig. 3*B*).

Cell cycle analysis using flow cytometry revealed that Bromodeoxyuridine (BrdU)-labeled S phase cells dramatically decreased when TS^{bip} cells were cultured at a high cell density (Fig. 3*C*). Both G1 and G2 arrest were responsible for the reduction of S phase cells (*SI Appendix*, Fig. S2 *A* and *B*). Cell density-dependent reduction of S phase cells was also observed in TS^{mole} cells, but to a much lesser extent than TS^{bip} cells (Fig. 3 *C* and *D*), reinforcing the idea that TS^{mole} cells have reduced sensitivity to contact inhibition. The cell cycle analysis also revealed that some TS^{mole} cell lines contained substantial proportions of cells >4n (Fig. 3*E* and *SI Appendix*, Table S1). As cells >8n were negligible, these lines were thought to contain mitotically active tetraploid cells (*SI Appendix*, Fig. S2*C*). The proportion of cells >4n was marginally reduced by increased cell density (*SI Appendix*, Fig. S2*D*). We found a significant relationship

($r = -0.72$, $P = 0.02$) between the proportion of cells >4n and cell doubling time (Fig. 3*F*), but the sample size was small, and further work is required to establish the negative correlation.

Identification of p57^{KIP2} as a Regulator of Contact Inhibition in TS Cells. We were next interested in why TS^{mole} cells had reduced sensitivity to contact inhibition. Abnormal expression of imprinted gene(s) is considered to be involved in this phenotype. We focused on *p57^{KIP2}* because this gene functions as a cyclin-dependent kinase inhibitor and was expressed at a very low level in TS^{mole} cells (Fig. 2*A*). Moreover, previous studies have revealed that p57^{KIP2} expression is absent or very low in CT cells of CHMs and the majority of choriocarcinoma samples associated with CHMs (17, 18). Although few TS^{bip} cells expressed p57^{KIP2} when they were cultured at a low density, p57^{KIP2} was strongly induced when cultured at a high density (Fig. 4 *A*–*C*). In contrast, p57^{KIP2}-positive cells were almost absent in TS^{mole} cells regardless of cell density. We also observed a ~30-fold induction of *p57^{KIP2}* mRNA in TS^{bip} cells cultured at a high density (Fig. 4*D*). Among the 14 imprinted genes labeled in Fig. 2*A*, *p57^{KIP2}* was most strongly induced by high cell density (Fig. 4*D* and *SI Appendix*, Fig. S3). These data suggest that transcriptional regulation may be an important determinant of the abundance of p57^{KIP2} in TS^{bip} cells, although we do not exclude the possibility of posttranscriptional regulation.

To determine whether loss of p57^{KIP2} expression is responsible for the reduced susceptibility to contact inhibition in TS^{mole} cells,
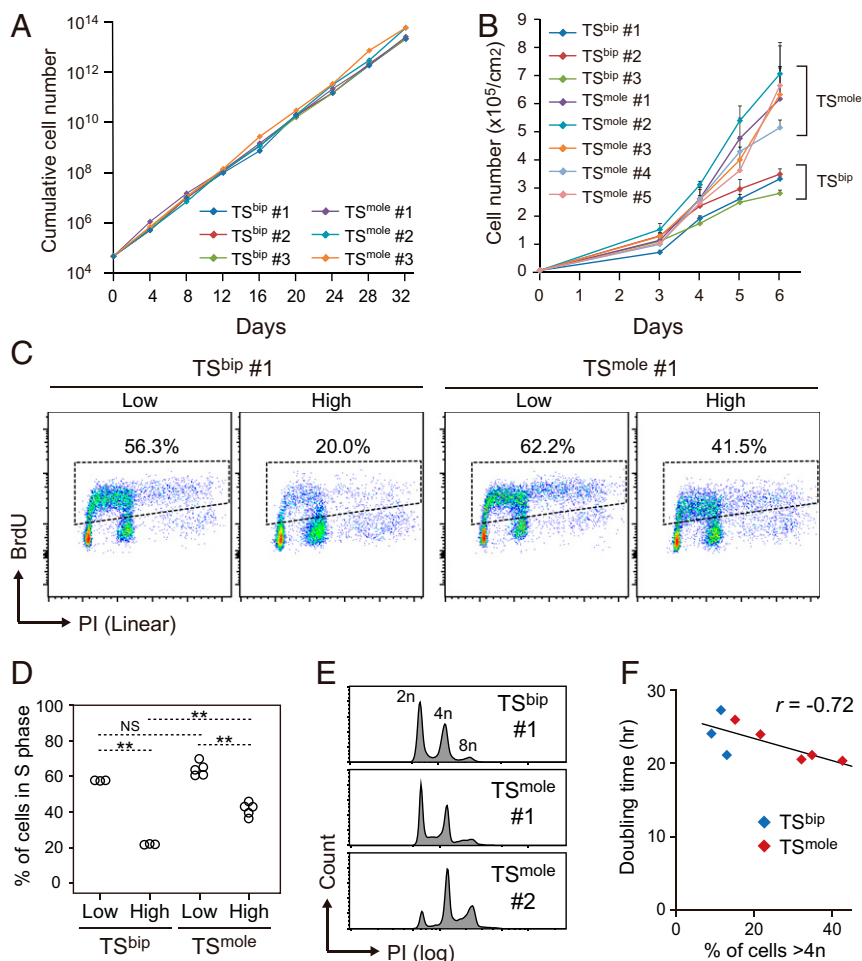
Fig. 3. Reduced sensitivity to contact inhibition in TS^mole cells. (*A*) Cumulative growth curves of TS^bip and TS^mole cells. Three TS^bip and three TS^mole cell lines were seeded at a density of 5,000 cells/cm². The cells were passaged when they reached ~80% confluence and counted every 4 d. (*B*) Growth curves of TS^bip and TS^mole cells. Three TS^bip and five TS^mole cell lines were analyzed. Cells were seeded at a density of 10,000 cells/cm² and maintained for 6 d without passaging. TS^mole cells had significantly higher cell numbers than TS^bip at day 6 ($P < 0.01$; Student's *t* test). Data are presented as means + SDs ($n = 3$). (*C*) Cell cycle analysis of TS^bip and TS^mole cells. Cells were seeded at a density of 5,000 (Low) or 100,000 cells/cm² (High). After 2 d of culture, the cells were labeled with BrdU for an hour and analyzed by flow cytometry. Nuclei were stained with PI. The proportions of cells in S phase are indicated. (*D*) Summary of the cell cycle analysis in *C*. Three TS^bip and five TS^mole cell lines were analyzed. Statistical analysis was performed by the Bonferroni/Dunn test. **$P < 0.01$; NS, not significant. (*E*) DNA ploidy analysis of TS^bip and TS^mole cells. DNA ploidy was measured using cells that were seeded at a high density (100,000 cells/cm²) and cultured for 2 d. (*F*) Relationship between DNA ploidy and cell doubling time. Three TS^bip and five TS^mole cell lines were analyzed and are shown in blue and red, respectively. A negative correlation was observed between cell doubling time during the exponential phase and the proportion of cells >4n, which was calculated from the data in *E*. Pearson's *r* was −0.72 ($P = 0.02$) when all samples were considered and −0.95 ($P = 0.05$) when only TS^mole samples were considered.

we utilized the doxycycline (Dox)-inducible Tet-on system (Fig. 5*A*). Three TS^mole cell lines with Dox-inducible *p57*^KIP2 were cultured at a high density, and their cell cycle was analyzed by flow cytometry. The fluorescence intensity of p57^KIP2 induced by Dox was comparable to that observed in TS^bip cells cultured at a high density (*SI Appendix*, Fig. S4*A*). We found that p57^KIP2 induction significantly reduced the proportion of cells in S phase (Fig. 5 *B* and *C*), which supports the idea that loss of p57^KIP2 confers resistance to contact inhibition in TS^mole cells. To reinforce this idea, we generated *p57*^KIP2 knockout TS cells using the CRISPR-Cas9 system. We transfected 1 TS^bip cells line with lentivirus-expressing Cas9 and gRNA and isolated 14 clones. Two of these were p57^KIP2-positive and the others were p57^KIP2-negative (Fig. 5*D*). One of the p57^KIP2-positive clones was wild type, and the other was heterozygous, implying that the paternal allele was mutated (*SI Appendix*, Fig. S4 *B* and *C*). These 2 lines were used as controls. We randomly selected 4 of the p57^KIP2-negative clones, which were all confirmed to be homozygous knockouts (*SI*

Appendix, Fig. S4*C*), and analyzed their proliferation. We found that at a high cell density, the proportion of S phase cells was much higher in p57^KIP2-negative clones than in p57^KIP2-positive clones (Fig. 5 *E* and *F*). Consistently, p57^KIP2-negative clones had higher proliferative activity than p57^KIP2-positive clones after reaching confluence (Fig. 5*G*). These data reveal that, similar to TS^mole cells, *p57*^KIP2 knockout TS cells have reduced sensitivity to contact inhibition. However, the proportion of cells >4n was comparable between p57^KIP2-negative and p57^KIP2-positive clones, suggesting that loss of p57^KIP2 may not be the cause of the genome amplification in TS^mole cells (Fig. 5*H*).

Discussion

Previous studies on mouse androgenetic cell lines have revealed important roles of genomic imprinting in cell proliferation. Similar to TS^mole cells, androgenetic mouse embryonic fibroblasts (MEFs) have increased saturation density (19). Interestingly, loss of p57 expression may not be involved in the
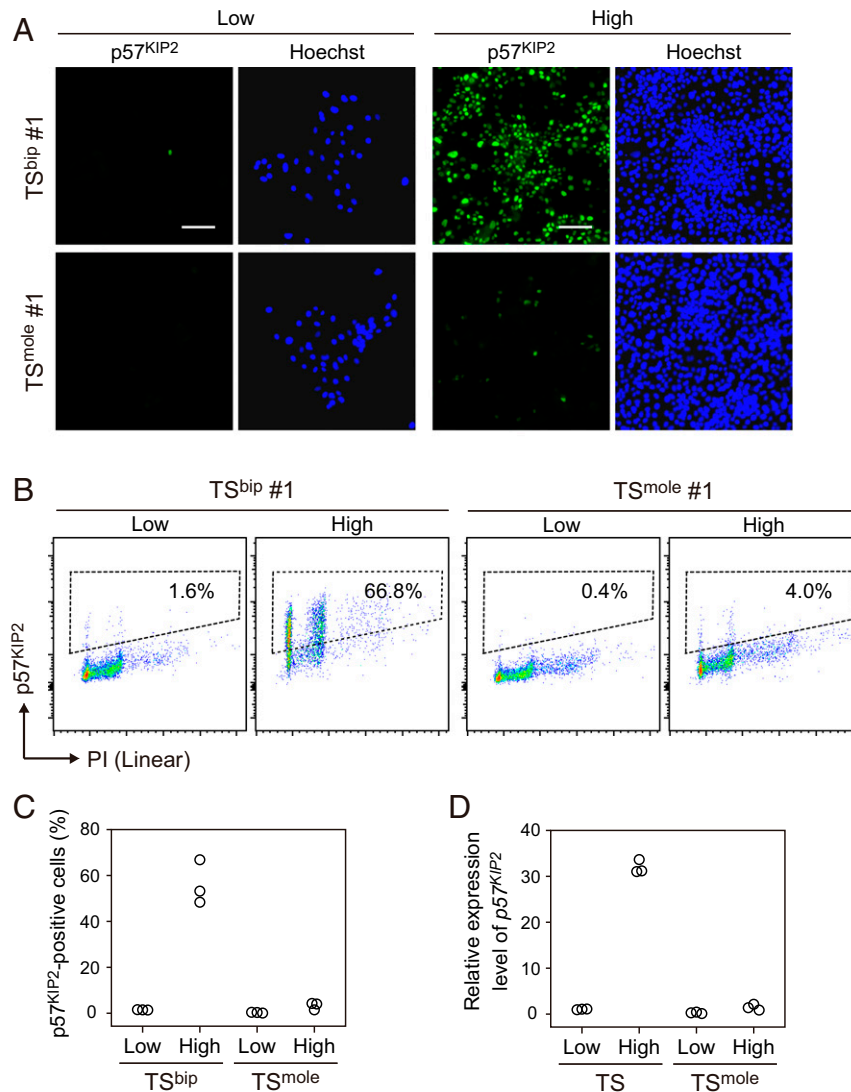
Fig. 4. Cell density-dependent induction of p57^{KIP2} in TS^{bip} cells but not in TS^{mole} cells. (*A*) Immunostaining images of p57^{KIP2} in TS^{bip} and TS^{mole} cells. Cells were seeded at a density of 5,000 (Low) or 100,000 cells/cm^2 (High). After 2 d of culture, cells were analyzed. Nuclei were stained with Hoechst 33258. (Scale bar: 100 μm.) (*B*) Flow cytometry analysis of p57^{KIP2} in TS^{bip} and TS^{mole} cells. Cells cultured as shown in *A* were analyzed. Nuclei were stained with PI. The proportions of p57^{KIP2}-positive cells are indicated. (*C*) Summary of flow cytometry analysis of p57^{KIP2} in *B*. Three TS^{bip} and three TS^{mole} cell lines were analyzed. (*D*) Expression levels of *p57^{KIP2}* in TS^{bip} and TS^{mole} cells. Three TS^{bip} and three TS^{mole} cell lines were cultured as shown in *A* and analyzed by quantitative real-time PCR. The data were normalized to *GAPDH* and *B2M*.

enhanced proliferation of androgenetic MEFs, because knockout of *p57^{KIP2}* has no effect on the proliferation of biparental MEFs. Alternatively, increased *Igf2* and loss of *Igf2r*, which is a maternally expressed imprinted gene and encodes a decoy receptor for IGF2, seem to stimulate the proliferation of androgenetic MEFs. It is also known that androgenetic mouse TS cells exhibit enhanced proliferation activity. Whereas biparental mouse TS cells require Fgf4 for their proliferation, androgenetic mouse TS cells continue to proliferate for up to 6 d in the absence of Fgf4 (20). Again, *p57^{KIP2}* is unlikely to be the major cause of the Fgf4-independent proliferation because p57^{KIP2} is expressed at similar levels in biparental and androgenetic mouse TS cells. *Gab1*, which is paternally expressed in the mouse placenta but not imprinted in the human placenta (21), is proposed to be a candidate gene for the Fgf4-independent proliferation (22). These findings suggest that although androgenesis is associated with enhanced cell proliferation, the underlying mechanisms may vary among tissues and species.

p57^{KIP2} is a putative tumor suppressor gene and most highly expressed in the placenta in both humans and mice (23, 24). Consistent with the function and expression pattern, *p57^{KIP2}*-deficient mice exhibit placentomegaly (25, 26) and loss of p57^{KIP2} function is associated with Beckwith–Wiedemann syndrome (BWS) in humans, which is characterized by overgrowth of multiple organs including the placenta (16, 27). However, it has been unclear how the expression and function of p57^{KIP2} are regulated in the placenta. We showed that p57^{KIP2} is strongly induced by increased cell density in TS^{bip} cells. This observation is consistent with the expression pattern of p57^{KIP2} in the placenta. The core mesenchyme of placental villi is surrounded by a single layer of proliferative CT cells that sporadically express p57^{KIP2} (28). At the tip of villi, CT cells form stratified aggregates known as cell columns, where they exit cell cycle and start to differentiate into extravillous cytotrophoblast (EVT) cells (29). p57^{KIP2} is strongly expressed in most CT cells that exit cell cycle and also in EVT cells (28). Therefore, increased cell
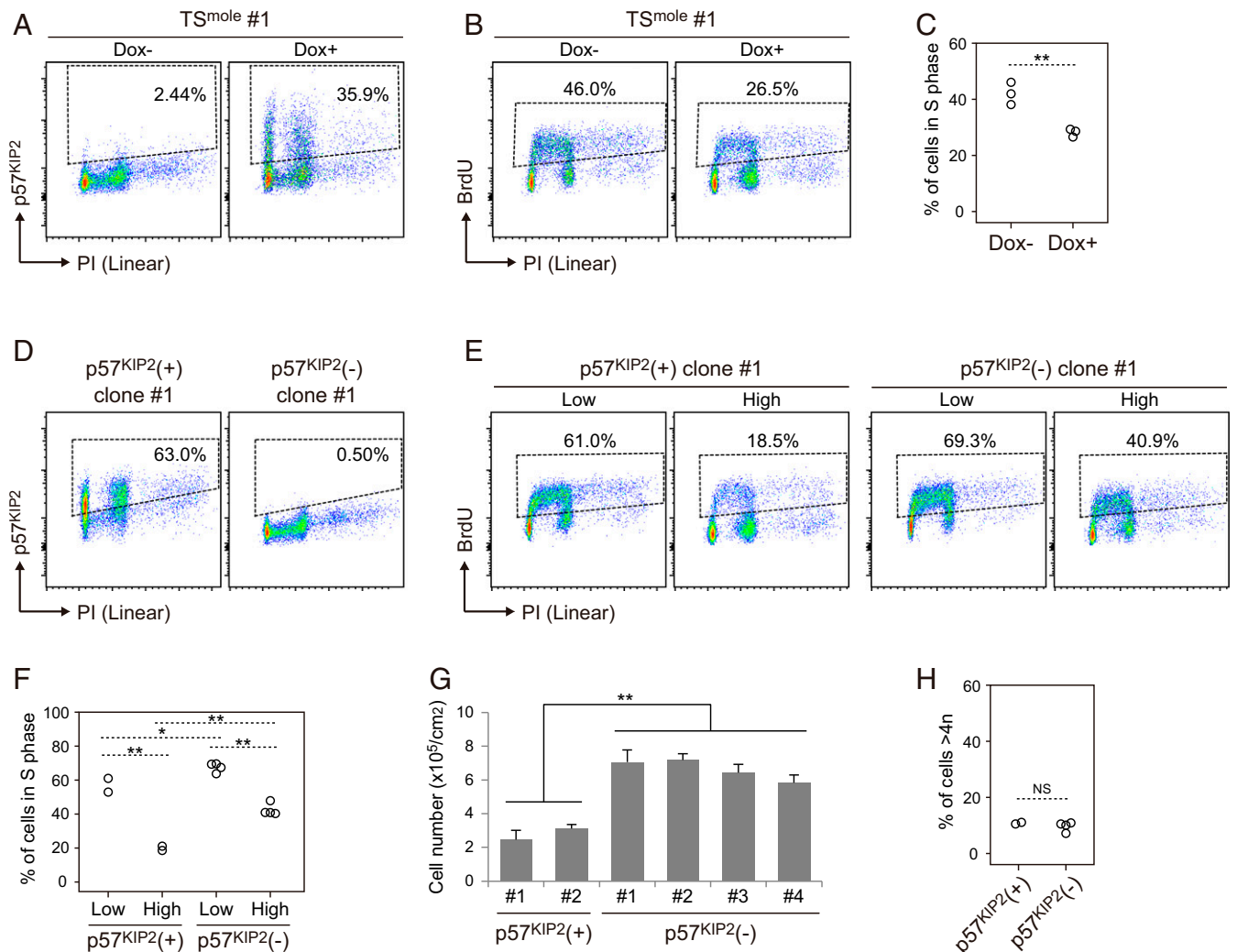
Takahashi et al.

Fig. 5. Identification of p57^{KIP2} as a regulator of contact inhibition in TS cells. (*A*) Overexpression of p57^{KIP2} in TS^{mole} cells. TS^{mole} cells with Dox-inducible p57^{KIP2} were seeded at a high density (100,000 cells/cm^2) and cultured for 24 h. Then, the cells were treated with 20 ng/mL Dox for 24 h, and p57^{KIP2} expression was analyzed by flow cytometry. Nuclei were stained with PI. The proportions of p57^{KIP2}-positive cells are indicated. Similar results were obtained with 3 independent TS^{mole} cell lines. (*B*) p57^{KIP2}-induced reduction of S phase cells. Cells were cultured as shown in *A* and analyzed by flow cytometry after BrdU treatment. Nuclei were stained with PI. The proportions of cells in S phase are indicated. (*C*) Summary of the cell cycle analysis in *B*. Three TS^{bip} and three TS^{mole} cell lines were analyzed. Statistical analysis was performed by Student's *t* test. **$P < 0.01$. (*D*) Confirmation of loss of p57^{KIP2} expression in *p57^{KIP2}* knockout clones. Cells were seeded at a high density (100,000 cells/cm^2). After 2 d of culture, p57^{KIP2} expression was analyzed by flow cytometry. The proportions of p57^{KIP2}-positive cells are indicated. Representative p57^{KIP2}-positive (+) and p57^{KIP2}-negative (−) clones are shown. (*E*) Cell cycle analysis of p57^{KIP2}(+) and p57^{KIP2}(−) clones. Cells were seeded at a low (5,000 cells/cm^2) or high density (100,000 cells/cm^2). After 2 d of culture, the cells were labeled with BrdU and analyzed by flow cytometry. The proportions of cells in S phase are indicated. (*F*) Summary of the cell cycle analysis in *E*. Two p57^{KIP2}(+) and four p57^{KIP2}(−) clones were analyzed. Statistical analysis was performed by the Bonferroni/Dunn test. **$P < 0.01$; *$P < 0.05$. (*G*) Reduced sensitivity to contact inhibition in p57^{KIP2}(−) clones. Cells were seeded at a density of 10,000 cells/cm^2 as in Fig. 3*B* and maintained for 5 d without passaging. TS^{mole} cells had significantly higher cell numbers than TS^{bip} cells ($P < 0.05$; Student's *t* test). Data are presented as means + SDs (n = 3). (*H*) Proportions of cells >4n in p57^{KIP2}(+) and p57^{KIP2}(−) clones. Two p57^{KIP2}(+) and four p57^{KIP2}(−) clones were analyzed. Statistical analysis was performed by Student's *t* test. NS, not significant.

density might be a trigger of p57^{KIP2} in vivo too. Our data strongly suggest that p57^{KIP2} is involved in cell cycle arrest in TS cells, but further studies are needed to determine whether p57^{KIP2} regulates permanent cell cycle exit and EVT differentiation.

Loss of p57^{KIP2} is observed in both CHMs and most BWS patients (16). Since malignant gestational trophoblastic neoplasms are not clinical characteristics of BWS, loss of p57^{KIP2} alone cannot account for the high risk of malignancy in CHMs. Polyploidy could be another risk factor. We found that some TS^{mole} cell lines contain high proportions of cells >4n, and the experiments presented suggest that loss of function of p57^{KIP2} is not responsible for that phenotype. Polyploid cells are also

observed in a subset of CHMs in vivo, and such CHMs are suspected to be prone to malignant gestational trophoblastic neoplasms (30, 31). Consistently, most invasive moles and choriocarcinomas exhibit genome amplification (32, 33). However, the frequency of CHMs containing polyploid cells is highly variable among studies, ranging from 2 to 30%, which may be due to inconsistent diagnostic criteria (34, 35). More studies using standardized criteria are needed to determine whether polyploidy is associated with malignant transformation in CHMs. Also, the mechanism underlying the polyploidization remains unknown.

In conclusion, we established and characterized TS^{mole} cells, which led to the identification of p57^{KIP2} as a regulator of

Takahashi et al.

contact inhibition. p57^{KIP2} is required for normal development of multiple organs, and loss of methylation of KvDMR1, which results in loss of p57^{KIP2} expression, is common in human adult tumors (36). Therefore, our findings could have broad implications in embryogenesis and tumorigenesis beyond CHMs.

Materials and Methods

Sample Collection. Placental samples were collected from patients after written informed consent was obtained. Experienced pathologists confirmed the diagnosis of CHMs. This study was approved by the Ethics Committee of Tohoku University Graduate School of Medicine (Research license 2017-1-349).

Culture of TS Cells. TS^{mole} cells were established as described previously (14). Briefly, CT cells were isolated from CHM tissues and cultured on plates coated with 5–10 μg/mL Col IV (Corning) using TS medium (DMEM/F12 [Wako] supplemented with 0.1 mM 2-mercaptoethanol [Wako], 0.2% FBS [Thermo Fisher Scientific], 0.5% Penicillin-Streptomycin [Thermo Fisher Scientific], 0.3% BSA [Wako], 1% ITS-X supplement [Wako], 1.5 μg/mL ʟ-ascorbic acid [Wako], 50 ng/mL EGF [Wako], 2 μM CHIR99021 [Wako], 0.5 μM A83-01 [Wako], 1 μM SB431542 [Wako], 0.8 mM VPA [Wako], and 5 μM Y27632 [Wako]). TS^{bip} #1, #2, and #3 were established in our previous study (14) and correspond to TS^{CT} #1, #2, and #3, respectively. TS^{bip} #4 was established in this study and used only for CNV analysis. Unless otherwise noted, we used TS^{mole} and TS^{bip} cells passaged 10–20 times for the analysis.

Overexpression of p57^{KIP2}. Vectors for Dox-inducible p57^{KIP2} expression were constructed as follows. The Tet-On 3G transactivator of the pTetOne vector (Takara) was PCR-amplified and cloned into the multicloning site of the CS-CA-MCS plasmid (kindly provided by H. Miyoshi, RIKEN BioResource Center, Ibaraki, Japan) using the In-Fusion HD Cloning kit (Takara). The resulting vector was designated as pCS-CA-Tet3G. The CAG promoter of CS-CA-MCS was replaced with the TRE3Gs promoter of pTetOne. The resulting vector was designated as pCS-3G. The coding region of p57^{KIP2} was PCR-amplified from cDNA prepared from TS^{bip} cells and cloned into pCS-3G to generate pCS-3G-p57^{KIP2}. Sequences of the primers used for vector construction are shown in Dataset S3.

To generate lentivirus expressing Tet-On 3G, pCS-CA-Tet3G was cotransfected with pCMV-VSV-G-RSV-Rev and pCAG-HIVgp (kindly provided by H. Miyoshi, RIKEN BioResource Center) into 293T cells using Lipofectamine LTX (Thermo Fisher Scientific). Ten micomolar Forskolin (Wako) was added after 24 h of transfection. The supernatant was collected after 3 d of transfection, concentrated with Lenti-X Concentrator (Takara), and stored at −80 °C. Lentivirus-expressing p57^{KIP2} was also generated using pCS-3G-p57^{KIP2}. TS^{mole} cells harboring Dox-inducible p57^{KIP2} were generated by adding lentivirus-expressing Tet-On 3G and p57^{KIP2} to the culture medium. p57^{KIP2} expression was induced by adding 20 ng/mL Dox for 24 h.

Knockout of p57^{KIP2}. Cas9 was amplified with PCR from the Alt-R S.p. Cas9 Expression Plasmid (IDT) and cloned into pCS-3G to generate pCS-3G-Cas9.

The CAG promoter of CS-CA-MCS was replaced with the human U6 (hU6) promoter, and the gRNA scaffold sequence was cloned downstream of the hU6 promoter. The resulting vector was designated as pCS-hU6. A gRNA target sequence for p57^{KIP2} (5′-GGC GAC AAG ACG CTC CAT CG-3′), which was designed and evaluated using CHOPCHOP (37), was cloned between the hU6 promoter and the gRNA scaffold to generate pCS-hU6-p57^{KIP2}.

Lentivirus-expressing Cas9 and the gRNA was prepared as described above and transduced into TS^{bip} cells. Cas9 was transiently expressed by adding 100 ng/mL Dox for 24 h, and single cells were cloned by limiting dilution. During lentivirus transduction and single-cell cloning, we cultured TS cells on plates coated with 0.5 μg/mL iMatrix-511 (Nippi) using a modified TS medium (DMEM/F12 supplemented with 1% KSR [Thermo Fisher Scientific], 0.5% Penicillin-Streptomycin, 0.15% BSA, 1% ITS-X supplement, 200 μM ʟ-ascorbic acid, 50 ng/mL EGF, 2 μM CHIR99021, 5 μM A83-01, 0.8 mM VPA, and 2.5 μM Y27632). This medium ameliorated the toxicity of lentivirus and improved cloning efficiency. Obtained clones were maintained in the original TS medium and analyzed by flow cytometry and Sanger sequencing. Sequences of the primers used for vector construction and Sanger sequencing are shown in Dataset S3.

External Data. The RNA-seq and WGBS data for TS^{bip} (Japanese Genotype-phenotype Archive [JGA] accession no. JGAS00000000117) and CT^{bip}, EVT^{bip}, and SynT^{bip} (JGA accession no. JGAS00000000038) were from our previous studies (14, 15).

Statistical Analyses. Results are presented as means + SDs. The statistical methods used are described in the figure legends. A P value of less than 0.05 was considered statistically significant. P values less than 0.05 and 0.01 were marked by 1 and 2 asterisks, respectively. Statistical analysis was performed using Statcel software (OMS) or R (version 3.3.1).

Other Methods. The procedures for immunostaining, CNV analysis, RNA-seq, real-time PCR, WGBS, and flow cytometory are provided in SI Appendix.

Data Availability. All sequencing data reported in this paper are available at JGA (accession no. JGAS00000000207) (38).

1. J. J. Candelier, The hydatidiform mole. *Cell Adhes. Migr.* **10**, 226–235 (2016).
2. V. Fock et al., Trophoblast subtype-specific EGFR/ERBB4 expression correlates with cell cycle progression and hyperplasia in complete hydatidiform moles. *Hum. Reprod.* **30**, 789–799 (2015).
3. M. J. Seckl, N. J. Sebire, R. S. Berkowitz, Gestational trophoblastic disease. *Lancet* **376**, 717–729 (2010).
4. T. Kajii, K. Ohama, Androgenetic origin of hydatidiform mole. *Nature* **268**, 633–634 (1977).
5. K. Ohama et al., Dispermic origin of XY hydatidiform moles. *Nature* **292**, 551–552 (1981).
6. A. Altieri, S. Franceschi, J. Ferlay, J. Smith, C. La Vecchia, Epidemiology and aetiology of gestational trophoblastic diseases. *Lancet Oncol.* **4**, 670–678 (2003).
7. A. C. Ferguson-Smith, Genomic imprinting: The emergence of an epigenetic paradigm. *Nat. Rev. Genet.* **12**, 565–575 (2011).
8. F. Zink et al., Insights into imprinting from parent-of-origin phased methylomes and transcriptomes. *Nat. Genet.* **50**, 1542–1552 (2018).
9. J. M. Frost, G. E. Moore, The importance of imprinting in the human placenta. *PLoS Genet.* **6**, e1001015 (2010).
10. J. McGrath, D. Solter, Completion of mouse embryogenesis requires both the maternal and paternal genomes. *Cell* **37**, 179–183 (1984).
11. M. A. Surani, S. C. Barton, M. L. Norris, Nuclear transplantation in the mouse: Heritable differences between parental genomes after activation of the embryonic genome. *Cell* **45**, 127–136 (1986).
12. K. M. Steinberg et al., Single haplotype assembly of the human genome from a hydatidiform mole. *Genome Res.* **24**, 2066–2076 (2014).
13. E. Yamamoto et al., Establishment and characterization of cell lines derived from complete hydatidiform mole. *Int. J. Mol. Med.* **40**, 614–622 (2017).
14. H. Okae et al., Derivation of human trophoblast stem cells. *Cell Stem Cell* **22**, 50–63.e6 (2018).
15. H. Hamada et al., Allele-specific methylome and transcriptome analysis reveals widespread imprinting in the human placenta. *Am. J. Hum. Genet.* **99**, 1045–1058 (2016).
16. T. Eggermann et al., CDKN1C mutations: Two sides of the same coin. *Trends Mol. Med.* **20**, 614–622 (2014).
17. M. Chilosi et al., Differential expression of p57kip2, a maternally imprinted cdk inhibitor, in normal human placenta and gestational trophoblastic disease. *Lab. Invest.* **78**, 269–276 (1998).
18. N. J. Sebire et al., p57(KIP2) immunohistochemical staining of gestational trophoblastic tumours does not identify the type of the causative pregnancy. *Histopathology* **45**, 135–141 (2004).
19. L. Hernandez, S. Kozlov, G. Piras, C. L. Stewart, Paternal and maternal genomes confer opposite effects on proliferation, cell-cycle length, senescence, and tumor formation. *Proc. Natl. Acad. Sci. U.S.A.* **100**, 13344–13349 (2003).
20. H. Ogawa et al., Cell proliferation potency is independent of FGF4 signaling in trophoblast stem cells derived from androgenetic embryos. *J. Reprod. Dev.* **62**, 51–58 (2016).
21. H. Okae et al., Re-investigation and RNA sequencing-based identification of genes with placenta-specific imprinted expression. *Hum. Mol. Genet.* **21**, 548–558 (2012).

22. D. Suzuki, H. Morimoto, K. Yoshimura, T. Kono, H. Ogawa, The differentiation potency of trophoblast stem cells from mouse androgenetic embryos. *Stem Cells Dev.* **28**, 290–302 (2019).

23. S. Matsuoka *et al.*, p57KIP2, a structurally distinct member of the p21CIP1 Cdk inhibitor family, is a candidate tumor suppressor gene. *Genes Dev.* **9**, 650–662 (1995).

24. M. H. Lee, I. Reynisdóttir, J. Massagué, Cloning of p57KIP2, a cyclin-dependent kinase inhibitor with unique domain structure and tissue distribution. *Genes Dev.* **9**, 639–649 (1995).

25. P. Zhang, C. Wong, R. A. DePinho, J. W. Harper, S. J. Elledge, Cooperation between the Cdk inhibitors p27(KIP1) and p57(KIP2) in the control of tissue growth and development. *Genes Dev.* **12**, 3162–3167 (1998).

26. K. Takahashi, T. Kobayashi, N. Kanayama, p57(Kip2) regulates the proper development of labyrinthine and spongiotrophoblasts. *Mol. Hum. Reprod.* **6**, 1019–1025 (2000).

27. S. J. Tunster, M. Van de Pette, R. M. John, Fetal overgrowth in the *Cdkn1c* mouse model of Beckwith-Wiedemann syndrome. *Dis. Model. Mech.* **4**, 814–821 (2011).

28. E. T. Korgun *et al.*, Location of cell cycle regulators cyclin B1, cyclin A, PCNA, Ki67 and cell cycle inhibitors p21, p27 and p57 in human first trimester placenta and deciduas. *Histochem. Cell Biol.* **125**, 615–624 (2006).

29. P. Bischof, I. Irminger-Finger, The human cytotrophoblastic cell, a mononuclear chameleon. *Int. J. Biochem. Cell Biol.* **37**, 1–16 (2005).

30. D. A. Martin *et al.*, DNA content as a prognostic index in gestational trophoblastic neoplasia. *Gynecol. Oncol.* **34**, 383–388 (1989).

31. H. Sugimori, Y. Kashimura, M. Kashimura, I. Taki, Nuclear DNA content of trophoblastic tumors. *Acta Cytol.* **22**, 542–545 (1978).

32. I. Nishiya, S. Moriya, K. Yamashita, T. Kikuchi, Cytophotometric DNA determination of trophoblastic neoplasia. *Gynecol. Oncol.* **5**, 103–108 (1977).

33. Y. Kashimura, A quantitative study of nuclear DNA of trophoblastic cells: Proliferation kinetics. *Gynecol. Oncol.* **16**, 374–382 (1983).

34. M. Fukunaga, Flow cytometric and clinicopathologic study of complete hydatidiform moles with special reference to the significance of cytometric aneuploidy. *Gynecol. Oncol.* **81**, 67–70 (2001).

35. L. Sundvall *et al.*, Tetraploidy in hydatidiform moles. *Hum. Reprod.* **28**, 2010–2020 (2013).

36. R. A. Scelfo *et al.*, Loss of methylation at chromosome 11p15.5 is common in human adult tumors. *Oncogene* **21**, 2564–2572 (2002).

37. T. G. Montague, J. M. Cruz, J. A. Gagnon, G. M. Church, E. Valen, CHOPCHOP: A CRISPR/Cas9 and TALEN web tool for genome editing. *Nucleic Acids Res.* **42**, W401–W407 (2014).

38. H. Okae, K. Kobayashi, Methylome and transcriptome profiling of CHM-derived TS cells. Japanese Genotype-phenotype Archive. https://ddbj.nig.ac.jp/jga/viewer/view/study/JGAS00000000207. Deposited 24 October 2019.

CELL BIOLOGY